Available online at www.sciencedirect.com
ScienceDirect
Journal of Sound and Vibration 323 (2009) 148–162
JOURNAL OF SOUND AND VIBRATION
www.elsevier.com/locate/jsvi

Bending-torsional flutter of wings with an attached mass subjected to a follower force

S.A. Fazelzadeh*, A. Mazidi, H. Kalantari

Mechanical Engineering Department, Shiraz University, Shiraz, Iran

Received 15 May 2008; received in revised form 29 December 2008; accepted 3 January 2009
Handling Editor: A.V. Metrikine
Available online 5 February 2009

Abstract

The bending-torsional flutter characteristics of a wing containing an arbitrarily placed mass under a follower force are presented. The governing equations and boundary conditions are determined via Hamilton's variational principle. In order to precisely consider the spanwise and chordwise locations and the properties of the attached external mass and the follower force, the generalized function theory is used. Unsteady aerodynamic pressure loadings are also considered. The resulting partial differential equations are transformed into a set of eigenvalue equations through the extended Galerkin's approach. The interactions cause the model differential equations of the problem to be non-self-adjoint. As a result, if each of the parameters flow speed, follower force, or external mass exceeds a certain critical value, the wing experiences flutter instabilities. The numerical results are also compared with the published results and excellent agreement is observed. Numerical simulations highlighting the effects of the follower force and the external mass parameters such as the mass ratio and the attached locations on the flutter speed and frequency are presented.
© 2009 Elsevier Ltd. All rights reserved.

1. Introduction

Flutter instability of elastic systems subjected to non-conservative forces has been studied by many authors. Bolotin has presented a book in which a general understanding of all the contributing factors in this area has been provided [1]. In this book, the lateral stability of a beam under the transverse follower force was analyzed first for a pinned configuration. The correlation between the stability and quasi stability regions of elastic and viscoelastic systems subjected to non-conservative forces was investigated by Bolotin and Zhinzher [2]. The equations for a cantilevered thin beam are derived by Kalmbach et al. [3]. They examined the possibility of controlling, through feedback, a thin-cantilevered beam subjected to a non-conservative follower force. The static and dynamic instabilities of a cantilevered beam and a simply supported plate under non-conservative forces have been studied by Zuo and Schreyer [4]. For the beam, instead of the two-degree-of-freedom model or a Galerkin approximation to the continuous model, the governing partial differential equation and associated boundary conditions of the continuous model have been solved exactly. Detinko [5] used a simple

*Corresponding author. Tel.: +98 711 613 3238; fax: +98 711 628 7508.
E-mail address: fazelzad@shirazu.ac.ir (S.A. Fazelzadeh).

0022-460X/$ - see front matter © 2009 Elsevier Ltd. All rights reserved.
doi:10.1016/j.jsv.2009.01.002

Nomenclature

b	wing semi chord
e	distance between center of gravity and elastic axis of the wing
E	young's modulus
G	shear modulus
H	heaviside function
$\hat{\mathbf{i}}, \hat{\mathbf{j}}, \hat{\mathbf{k}}$	unit vectors of undeformed wing coordinate system
$\hat{\mathbf{i}}', \hat{\mathbf{j}}', \hat{\mathbf{k}}'$	unit vectors of deformed wing coordinate system
I	wing cross-section moment of inertia
J	wing cross-section polar moment of inertia
k_m	mass radius of gyration
l	wing length
L	wing sectional lift
m	mass of the wing per unit length
m_s	density of the external mass
M	aerodynamic moment
M_s	external mass
M_s^*	non-dimensional external mass
p	non-dimensional follower force
$\mathbf{R_S}$	external mass displacement vector
T	kinetic energy
U	strain energy
U_∞	air stream velocity
v_∞	non-dimensional flow speed
v_f	non-dimensional flutter speed
w	displacement in z direction
x, y, z	undeformed wing coordinate system
x', y', z'	deformed wing coordinate system
x_s, y_s, z_s	the external mass location in x, y and z directions, respectively
X_s, Y_s	non-dimensional external mass location in x, y directions, respectively
δ	variational operator
δ_D	dirac delta function
ε_{ij}	strain component
θ	twist angle
λ	bending rigidity (EI)/ torsion rigidity (GJ)
ρ	density of the wing
ρ_∞	air density
σ_{ij}	stress component
ω_f	flutter frequency
ω_θ	torsional frequency

model of a slender beam loaded by a transverse follower force to show that the lateral stability analysis of a beam under the follower load should include slight internal and realistic external damping to avoid the overestimation of the critical load. Nair et al. [6] studied the stability of a short uniform column subjected to an intermediate follower force. They showed the necessity of using Timoshenko's beam model when the follower force is very near to the support. The effects of non-conservative forces on the elastic stability of the structures have been studied in all of the previously mentioned works. Indeed, much of the research in this field has focused on the stability of the structures subjected to different types of non-conservative forces, and there is a limited amount of literature concerned with the aeroelastic stability of such structures available.

It is well known that aeroelastic instability may be induced in elastic systems because of non-conservative forces. The high-thrust engine mounted on the aircraft wing is a good example of acting non-conservative forces on the airplane structure. One of the most dramatic aeroelastic phenomenons is flutter, a dynamic instability that often leads to terrible structural failure in airplane components. Due to the fact that nowadays the importance of weight saving in flight vehicles increases the structural flexibility of the aircraft, the effects of the thrust and engine mass on the flutter speed could be considerable.

Many of the previous efforts made to simulate wing flutter have considered uniform straight wings, both with and without external stores. One of the first works in this field is the paper by Goland [7], which concentrated on the flutter speed determination of a uniform cantilever wing. He verified the flutter speed by integration of the differential equations of the wing motion. This work was then continued on a uniform wing with tip weights [8]. Runyan and Watkins [9] analyzed the flutter of a uniform wing and made a comparison between the analytical and the experimental results. The aeroelastic stability of a swept wing with tip weights for an unrestrained vehicle has been considered by Lottati [10]. In his work a composite wing was studied and it was observed that flutter occurs at a lower speed as compared to a clean wing configuration. Gern and Librescu have made some efforts to show the effects of externally mounted masses on the static and dynamic aeroelasticity of advanced swept cantilevered wings [11,12]. The dynamic response of adaptive cantilevered

beams carrying externally mounted stores and exposed to time-dependent external excitations has been considered by Na and Librescu [13]. Moreover, Librescu and Song [14] investigated the free vibration and dynamic response to external time-dependent loads of aircraft wings carrying eccentrically located heavy stores. They have modeled the wing as a thin-walled anisotropic composite beam.

It seems that the stability problem of a cantilever wing containing a mass excited by a transverse follower force has not received much attention in the literature. Como [15] analyzed the bending-torsional stability of a cantilevered beam subjected at its end section to a lateral follower force. In his work the distributed mass and inertia properties of the beam were neglected, although a concentrated mass and inertia at the tip were included. Feldt and Herrmann [16] investigated the flutter instability of a wing containing a mass subjected to the transverse follower force at the wing tip in the presence of airflow. Only one value of the bending stiffness to torsional stiffness ratio was considered in their study, a value for which thrust is destabilizing. Moreover, their results generally did not agree with previous works. Hodges et al have shown the effects of the lateral follower force on flutter boundary and the frequency of distributed cantilever wings [17,18]; however, they did not take into account the external concentrated mass effects.

To add to the aforementioned bulk of literature in this field, the aeroelastic modeling and flutter study of the wings containing an arbitrarily placed mass subjected to a follower force is considered in this study. Furthermore, discussions about the combined effects of the follower force and external mass in conjunction with airflow on the flutter speed and frequency are presented.

2. Problem statement

The cantilever wing containing a mass subjected to a lateral follower force as shown in Fig. 1 is considered. In Fig. 1a, the undeformed wing is illustrated. Likewise, the wing typical section is represented in Fig. 1b,

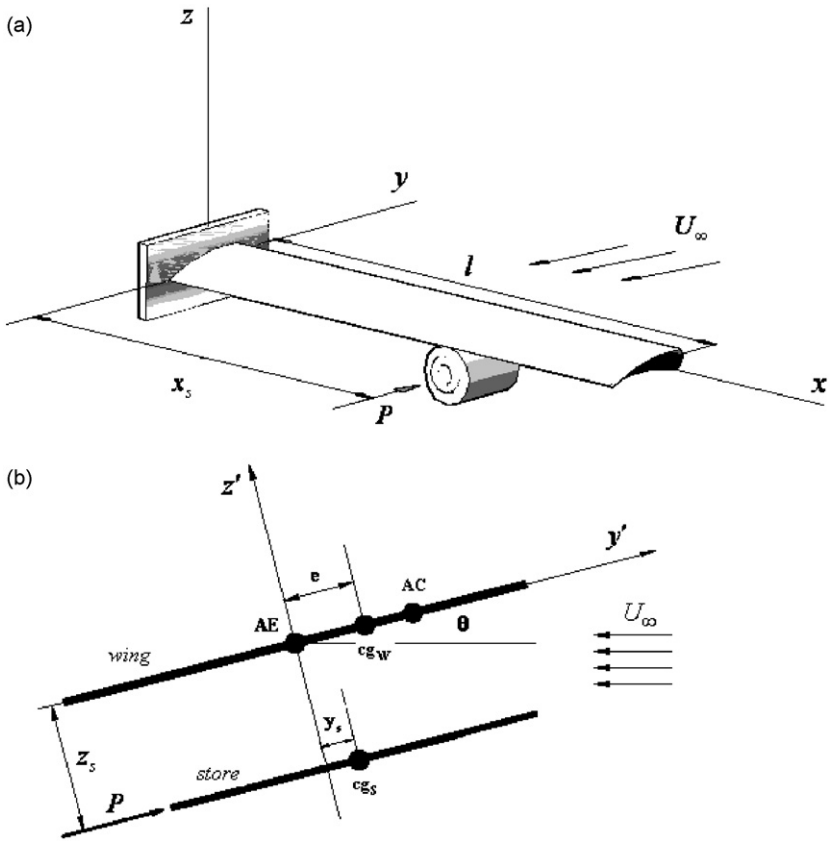

Fig. 1. (a) The wing/store configuration under follower force and (b) the deformed wing/store section.

where y_s and z_s are the distances between the center of gravity of the external mass and the elastic axis of the wing. Also, points AE, AC, cg_w and cg_s refer to the wing elastic axes, aerodynamic center of the wing, wing center of gravity and store center of gravity, respectively.

The wing performs as a thin beam and the structural model, which incorporates bending-torsion flexibility, is used. The external mass inertia as well as the follower force are accounted for in deriving the governing equations. The equations of motion to be derived are valid for long, straight, homogeneous, isotropic wings. Because of the wing flexibility two coordinate systems have been used here. As shown in Fig. 1, the orthogonal axes x, y, z are fixed on an airplane base body in which the x axis lies in the spanwise direction. The other coordinate system, x', y', z', has been fixed on a deformed wing. After the wing deformation, the shear center of the cross-section located at x is displaced by an amount of w in z direction. Additionally, the angle of twist of the cross-section changes to θ about the x axis.

The coordinate transformation should be used between these two coordinates to derive the governing equations [19]:

$$\begin{Bmatrix} \hat{\mathbf{i}}' \\ \hat{\mathbf{j}}' \\ \hat{\mathbf{k}}' \end{Bmatrix} = \begin{bmatrix} 1 & 0 & w' \\ 0 & 1 & \theta \\ -w' & -\theta & 1 \end{bmatrix} \begin{Bmatrix} \hat{\mathbf{i}} \\ \hat{\mathbf{j}} \\ \hat{\mathbf{k}} \end{Bmatrix} \tag{1}$$

3. Governing equations

The equations of motion and boundary conditions are derived using Hamilton's variational principle that may be expressed as [20]:

$$\int_{t_1}^{t_2} [\delta U - \delta T_w - \delta T_s - \delta W]\,\mathrm{d}t = 0 \quad \delta w = \delta\theta = 0 \ \text{ at } t = t_1 = t_2 \tag{2}$$

where U and T are strain energy and kinetic energy, and W is the work done by non-conservative forces. The indices w and s identify the wing and externally mounted mass, respectively. The kinetic energy of the wing is simply [18]:

$$T_w = \frac{1}{2}\int_0^l \int \int_A \rho(\dot{w}^2 + k_m^2\dot{\theta}^2 + 2me\dot{\theta}\dot{w})\,\mathrm{d}x\,\mathrm{d}A \tag{3}$$

Herein, k_m is the radius of gyration and $(\dot{\cdot})$ is the partial derivative with respect to time. The first variation of kinetic energy can be recast as follows:

$$\delta T_w = \int \{(-m\ddot{w} - me\ddot{\theta})\delta w + (-mk_m^2\ddot{\theta} - me\ddot{w})\delta\theta\}dx \tag{4}$$

Using the kinematical procedure, the kinetic energy of the external mass can be derived. After deformation, the position vector of an arbitrary point on the external mass is

$$\mathbf{R_S} = x_s\hat{\mathbf{i}} + w\hat{\mathbf{k}} + (y_s + \eta)\hat{\mathbf{j}}' + (z_s + \xi)\hat{\mathbf{k}}' \tag{5}$$

In this equation x_s, y_s and z_s denote the external mass location in x, y and z directions, respectively. Also, η and ξ are the distances between such arbitrary point and the center of gravity of the external mass in y' and z' directions, respectively. Now, the kinetic energy of the external mass can be derived as

$$T_s = \frac{1}{2}\int_0^l \int \int_{A_s} m_s(\dot{\mathbf{R}}_\mathbf{S}\cdot\dot{\mathbf{R}}_\mathbf{S})\delta_D(x - x_s)\,\mathrm{d}A_s\,\mathrm{d}x \tag{6}$$

where m_s is the density of the store and A_s is the external mass cross-section area. Substituting Eqs. (1) and (5) and Eq. (5) in Eq. (6), taking the first variation results in

$$\delta T_s = \int_0^l \{M_s(z_s^2\ddot{w}''\delta w - (z_s^2 + y_s^2)\ddot{\theta}\delta\theta - \ddot{w}\delta w - y_s\ddot{w}\delta\theta - y_s\ddot{\theta}\delta w) + I_{M_s}\ddot{\theta}\delta\theta\}\delta_D(x - x_s)\,\mathrm{d}x \tag{7}$$

I_{M_s} denotes the external mass moment of inertia from the external mass centroidal x axes and M_s represents the external mass. The strain energy is considered next. The first variation of the strain energy is

$$\delta U = \int_V [\sigma_{22}\delta\varepsilon_{22} + \sigma_{12}\delta\varepsilon_{12} + \sigma_{23}\delta\varepsilon_{23}]\,\mathrm{d}x\,\mathrm{d}A \tag{8}$$

herein σ_{ij} and ε_{ij} are stress and strain components, respectively, and can be obtained directly from the displacement field [19]. Substituting these components, Eq. (8) can be recast as

$$\begin{aligned}\delta U = \int_0^l \{&[-GJ\theta'' + P(x_s - x)H(x_s - x)w'']\delta\theta + [EIw'''' + P(x_s - x)H(x_s - x)\theta''\\ &- 2P\theta' H(x_s - x)]\delta w\}\,\mathrm{d}x + [GJ\theta'\delta\theta + EIw''\delta w' - EIw'''\delta w + P(x_s - x)H(x_s - x)\theta\delta w'\\ &- [P(x_s - x)H(x_s - x)\theta]'\delta w]_0^l\end{aligned} \tag{9}$$

where H is Heaviside function. The virtual work of non-conservative forces acting on the wing may be expressed as

$$\delta W = \delta W_A + \delta W_F \tag{10}$$

δW_A is the virtual work of aerodynamic forces acting on the wing

$$\delta W_A = \int_0^l (L\delta w + M\delta\theta)\,\mathrm{d}x \tag{11}$$

Table 1
Characteristics of the wing/store model.

Parameters	Value
Length	1.2192 m
Semi-chord	*0.1016 m*
Bending rigidity	403.76 N m^2
Torsional rigidity	198.58 N m^2
Mass per unit length	*1.2942 kg m^{-1}*
Moment of inertia	*0.0036 kg m*
Spanwise elastic axis	*43.7% chord*
Center of gravity of wing	*45.4% chord*
Air density	1.224 kg m^{-3}
External mass	*1.578 kg*
Store moment of inertia	*0.0185 kg m^2*

Table 2
Validation of flutter speed and frequency for wing/store without follower force.

Location of the store (m)	Numerical Ref. [9]		Experimental Ref. [9]		Present					
	U_f (m/s)	ω_f (Hz)	U_f (m/s)	ω_f (Hz)	U_f (m/s)	Error respect to numerical (%)	Error respect to experimental (%)	ω_f (Hz)	Error respect to numerical (%)	Error respect to experimental (%)
0	101.50	25.27	101.80	22.10	98.67	−2.79	−3.07	24.58	−2.73	11.22
0.2794	100.89	19.23	98.75	17.40	96.16	−4.69	−2.62	19.58	1.82	12.53
0.4318	124.05	28.04	116.43	26.80	119.81	−3.42	2.9	28.15	0.39	5.04
0.7620	160.32	30.68	–	–	159.5	−0.51	–	30.8	0.39	–
1.1430	122.22	25.67	–	–	117.2	−4.11	–	26.05	1.48	–
1.1684	112.17	24.87	112.17	21.80	108.07	−3.66	−3.66	25.394	2.11	16.49
1.2192	91.44	23.60	97.54	21.40	92.83	1.52	−4.83	24.39	3.35	13.97

where L and M are aerodynamic lift and moment, respectively. These aerodynamic loads will be discussed later. The virtual work also contains effects associated with the follower force that may be caused by the release of a rocket or the motor thrust force. δW_F is the virtual work caused by such follower force and can be

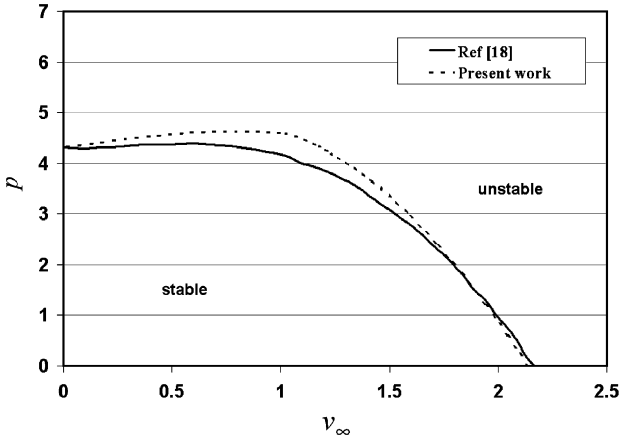

Fig. 2. Validation of flutter boundary.

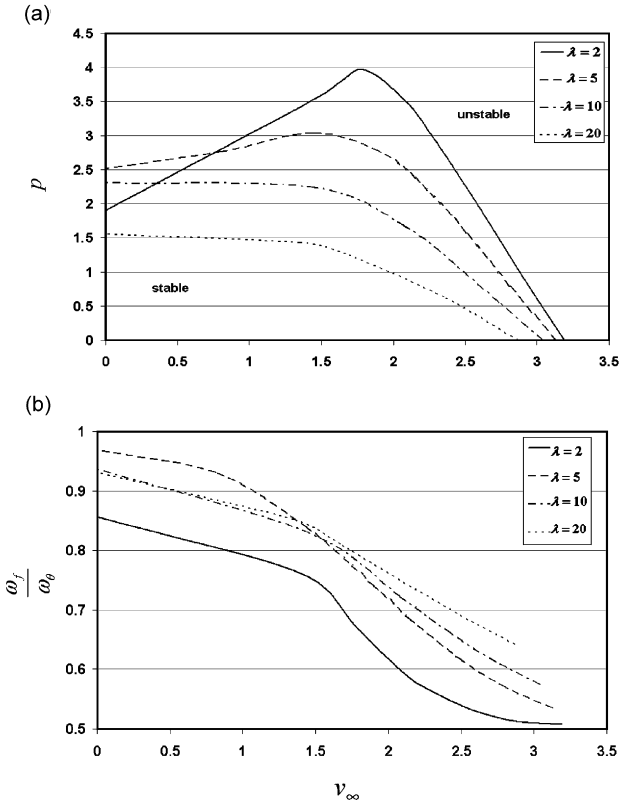

Fig. 3. Effects of λ on the wing critical behavior for $X_s = 1$, $Y_s = 0$ and $M_s^* = 0$: (a) flutter boundaries and (b) corresponding flutter frequencies.

derived as

$$\delta W_F = \int_0^l \{[P\theta\delta(x-x_s)]\delta w + [(Py_s\theta - Pz_s)\delta_D(x-x_s)]\delta\theta\}\,\mathrm{d}x \tag{12}$$

where P is the follower force. Substituting Eqs. (4), (7), (9), (10), (11) and (12) in Eq. (2), and noticing that for every admissible variation $(\delta w, \delta\theta)$ the coefficient of these variations must be zero, the aeroelastic governing equations are obtained as

$$m\ddot{w} + me\ddot{\theta} + EIw'''' + P(x_s - x)H(x_s - x)\theta'' - 2P\theta' H(x_s - x) + [M_s\ddot{w} + M_s y_s\ddot{\theta} - M_s z_s^2\ddot{w}'' - P\theta]\delta_D(x_s - x)\} = L \tag{13}$$

$$mk_m^2\ddot{\theta} + me\ddot{w} - GJ\theta'' + P(x_s - x)H(x_s - x)w'' + [M_s y_s\ddot{w} + (I_{M_s} + M_s(z_s^2 + y_s^2))\ddot{\theta} + Pz_s - Py_s\theta]\delta_D(x_s - x)\} = M \tag{14}$$

In these equations the Heaviside and Dirac delta functions are used in order to precisely consider the location and properties of the lateral follower force and the attached mass, respectively, and the index s identifies the affiliation of the respective quantity to the external mass. It is important to note in these equations the assumption that the follower force will act on the external mass, and applies directly to the chordwise direction of the wing. L and M are unsteady aerodynamic lift and moment as

$$L = -\pi\rho_\infty b^3\omega^2[l_w\overline{w}/b + l_\theta\overline{\theta}] \tag{15}$$

$$M = \pi\rho_\infty b^4\omega^2[m_w\overline{w}/b + m_\theta\overline{\theta}] \tag{16}$$

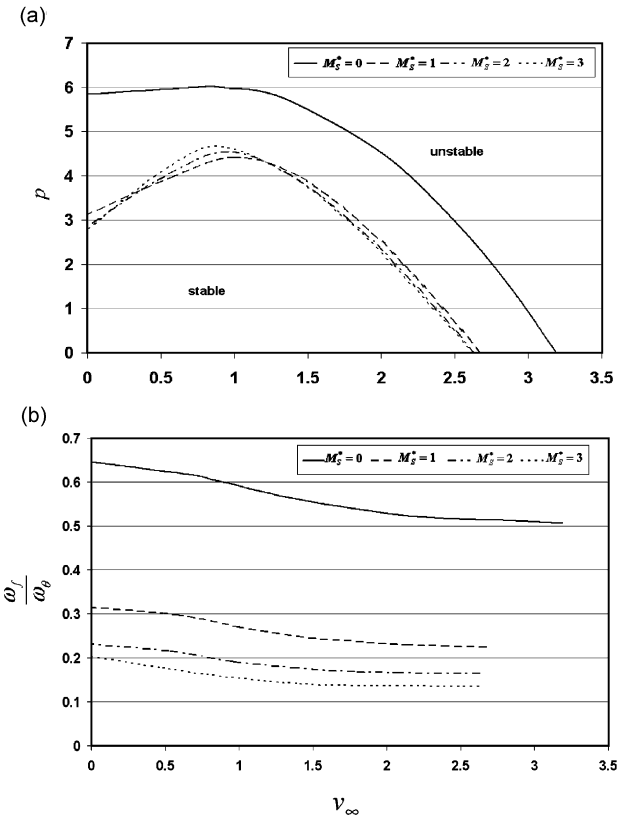

Fig. 4. Effects of M_s^* on the wing critical behavior for $X_s = 0.8$, $Y_s = 0$: (a) flutter boundaries and (b) corresponding flutter frequencies.

In Eqs. (15), (16) l_w, l_θ, m_w and m_θ are the aerodynamic coefficients as displayed by Hodges and Pierce [21], and ω and $\overline{w}, \overline{\theta}$ are the frequency, the plunge and the pitch amplitude of the harmonic motion, respectively.

Assuming that the wing can be represented by a cantilever beam, the boundary conditions are as follows: at $x = 0$, that is at the root of the wing, the deflection and slope are both zero (clamped end); at $x = l$, that is at the wing tip, moment and shear forces are both zero (free end). By using these boundary conditions the aeroelastic governing equations will be solved.

4. Method of solution

Due to the intricacy of the aeroelastic governing equations, the solution is searched by using an approximate solution procedure. To this end, w, θ are represented by means of a series of trial functions, φ_i, that should satisfy the boundary conditions, and multiplied by time dependent generalized coordinates, $\mathbf{q}_i$. Consequently, the displacement quantities are expressed as

$$w = \varphi_1^{\mathrm{T}} \mathbf{q}_1, \quad \theta = \varphi_2^{\mathrm{T}} \mathbf{q}_2 \tag{17}$$

Due to the complex boundary conditions and complex couplings involved in the above equations, it is difficult to generate proper comparison functions that fulfill all the geometric and natural boundary conditions. Therefore, in order to solve the above equations in a general way, the extended Galerkin's method is used [22]. The underlying idea of this method is to select weight functions that need only fulfill the geometric boundary conditions, while the effects of the natural boundary conditions are kept in the governing equations. When the linear combination of these weight functions is capable of satisfying the natural boundary conditions, the convergence rate is usually excellent.

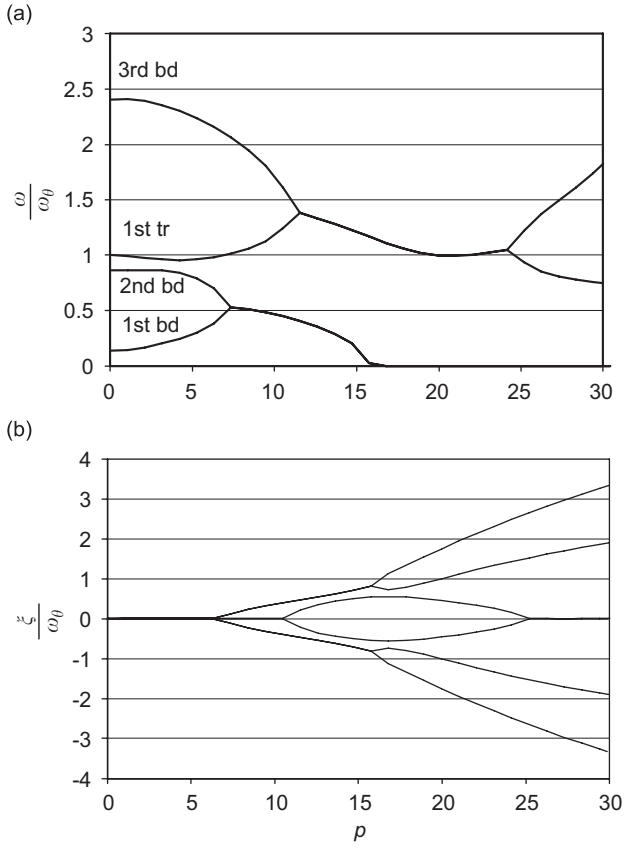

Fig. 5. (a) Frequency and (b) damping ratios vs. follower force for $X_s = 1$, $Y_s = 0$ and $M_s^* = 0$.

The following family of orthogonal functions for w and θ is used here based on the above remarks [21]:

$$\varphi_{1i} = \frac{(x/l)^{1+i}\{6 + i^2(1-x/l)^2 + i[5 - 6x/l + (x/l)^2]\}}{i(1+i)(2+i)(3+i)}$$

$$\varphi_{2i} = \mathrm{Sin}\left(\frac{i\pi x}{l}\right) \tag{18}$$

By substituting Eqs. (15)–(18) in Eqs. (13), (14), applying the Galerkin procedure on the governing equations, and by using orthogonal properties in the required integrations, the following set of ordinary differential equations are obtained:

$$[\mathbf{M}]\ddot{\mathbf{q}} + [\mathbf{K}]\mathbf{q} = \mathbf{Q}_{\mathrm{n.c}} \tag{19}$$

Herein, [**M**], [**K**] and $\mathbf{Q}_{\mathrm{n.c}}$ denote the mass matrix, stiffness matrix and non-conservative load vector, respectively, while **q** is the overall vector of the generalized coordinates. This representation finally leads to a complex eigenvalue problem expressed in matrix form as

$$\mathbf{A} - \omega^2\mathbf{B} = 0 \tag{20}$$

where **A** denotes the (real) stiffness matrix of the wing and **B** is the (complex) matrix representing the inertia terms of the wing and external mass, as well as the complex aerodynamic parameters. The real part of the complex valued quantity ω represents the circular frequency of the oscillation, whereas its imaginary part constitutes the damping factor. The implemented solution methodology, as discussed in Ref. [12], is based on the inversion of the complex matrix **B** and the subsequent calculation of complex eigenvalues and eigenvectors

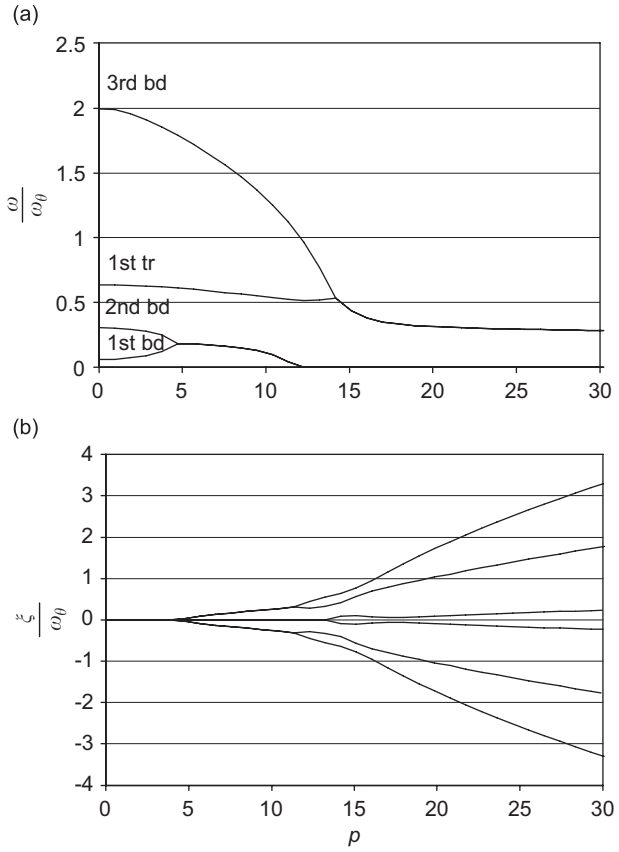

Fig. 6. (a) Frequency and (b) damping ratios vs. follower force for $X_s = 1$, $Y_s = 0$ and $M_s^* = 1$.

of the obtained system matrix $\mathbf{AB}^{-1}$. The flutter speed is calculated in a converging iteration process, rendering zero the imaginary (damping) part of the complex eigenvalues.

5. Numerical results and discussion

As stated in the previous section, the solution to this aeroelastic problem through the extended Galerkin method is sought by using a numerical integration scheme. Five bending modes and three torsion modes are considered in the solution procedure to this end. The effects of the external mass and the follower force value and location on the flutter speed of cantilever wings are simulated. Relevant data for the particular wing-weight combination used here are the same as those utilized in Ref. [9] and are considered in Table 1. Dimensionless parameters used in the numerical simulation are

$$\lambda = \frac{EI}{GJ}, \quad p = \frac{Pl^2}{\sqrt{GJEI}}, \quad M_s^* = \frac{M_s}{ml}, \quad v_\infty = \frac{U_\infty}{b\omega_\theta}, \quad v_f = \frac{U_f}{b\omega_\theta}, \quad X_s = x_s/l, \quad Y_s = y_s/b$$

Here, the vertical distance between the center of gravity of the external mass and the elastic axis of the wing is equal to zero.

In Table 2, for the purpose of validating the results in the absence of the follower force, is compared with Ref. [9] for different spanwise locations of the external mass, and good agreement with the theoretical and experimental results is observed. Furthermore, for the purpose of model validation the results for the wing without external mass are compared in Fig. 2 with Ref. [18] and good agreement is reported. Small differences come from the fact that the Theodorsen model is used here instead of Peter's model, which was used in Ref. [18]. Also, the same wing characteristics used in this reference are selected for model validation. In this

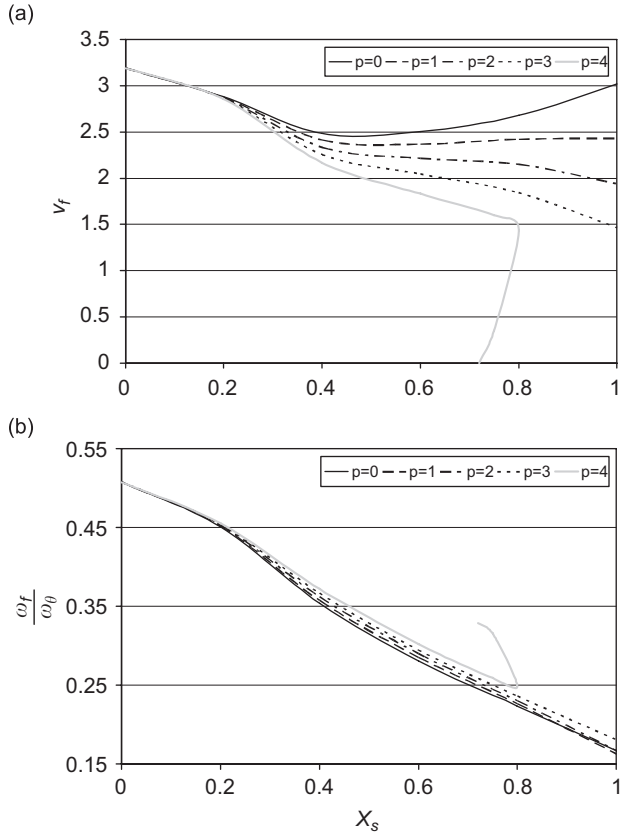

Fig. 7. Effects of the spanwise position of the follower force and external mass on the wing critical boundary for $Y_s = 0$ and $M_s^* = 1$: (a) flutter speed and (b) flutter frequencies.

figure the flutter boundary for $\lambda = 10$ is illustrated. A continued decrease in the flutter speed accompanying the increase in the follower force is seen. This can be explained, as the addition of the follower force destabilizes the wing and leads to instability at lower speeds.

Fig. 3 shows a parametric study investigating the effect of λ on the flutter boundary and the flutter frequency corresponds to this boundary for the clean wing. There is a continuous decrease in the magnitude of the thrust required for instability with an increase in airspeed. This happens because the destabilizing effect of the aerodynamic forces is added to the system, leading to instability at lower levels of the follower force. It is obvious that the stability region is quite different for lower values of λ as compared to the higher ones. This comes from the interactions between the thrust and aeroelastic destabilization mechanism. It can also be seen that, for larger values of air speed, the flutter occurs at lower frequencies.

The effect of external mass on the flutter boundary and corresponding flutter frequency of the wing is illustrated in Fig. 4. The external mass is assumed to be placed at the tip and precisely on the elastic axis of the wing. It can be seen that the stability region of the wing is limited when the external mass is attached to it. This is almost independent of the mass ratio parameter M_s^*. For low values of air speed the flutter speed increases, but when the air speed is increased further, the mode of instability changes from a dominant follower force mode to dominant aeroelastic instability.

The frequency and damping of the clean wing affected by a tip follower force are sketched in Fig. 5 for $M_s^* = 0$. It can be seen from Fig. 5(a) that the flutter occurred due to the intersection of the first bending mode with the second bending mode. It is clear from Fig. 5(b) that the corresponding damping for this point is zero. Fig. 6 shows the frequency and damping for the same configuration of the wing with $M_s^* = 1$. It can be understood from this figure that, as the store mass becomes greater, the intersection point corresponding to

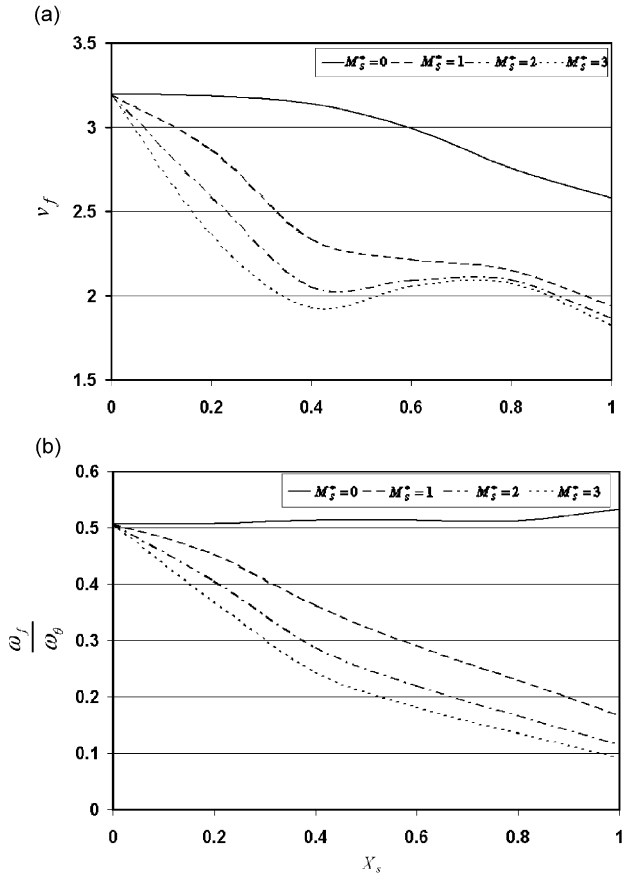

Fig. 8. Effects of the spanwise position of the follower force and external mass on the wing critical boundary for $Y_s = 0$ and $p = 2$: (a) flutter speed and (b) flutter frequencies.

the flutter condition moves to the left. This means that flutter occurs in smaller values of the follower force and the stability region is limited.

The influence of the spanwise location of the external mass on the flutter speed and frequency of the wing for selected values of the follower force is shown in Fig. 7. It is important to note that the follower force acts on the external mass and applies directly to the chordwise direction of the wing. In this case the mass ratio is $M_s^* = 1$. In the absence of the follower force, the lowest value of the flutter speed takes place around $X_s = 0.6$. So, one can say that this point is the critical location for store mounting for this wing characteristic. This behavior is also observed by Gern and Librescu [12]. In addition to the follower force, it can be seen in this figure that increasing the distance of the external mass from the wing root will decrease the flutter speed. This is more apparent for greater values of the follower force. For $p = 4$, an unusual behavior is observed. This can be qualitatively explained as the increase of the destabilizing effect of the follower force leading to instability, even at zero air speed. Fig. 7 also reveals that the flutter frequency drops in the usual way by moving the external mass and its follower force towards the wing tip. The magnitude of the follower force has no noticeable influence on the flutter frequency.

Dimensionless flutter speed and frequency of the wing are sketched in Fig. 8 versus the dimensionless spanwise location of the external mass for several values of the mass ratio. The external mass is mounted on the elastic axis and the dimensionless follower force is $p = 2$. It is clear from the figure that increasing the store mass decreases the flutter speed and the flutter frequency of the wing. It is important to notice that, although the results subjected to each mass ratio are unique, the trend of the results is the same for all cases. Moving outward the external mass for all mass values lowers flutter frequencies. So it can be observed that in the

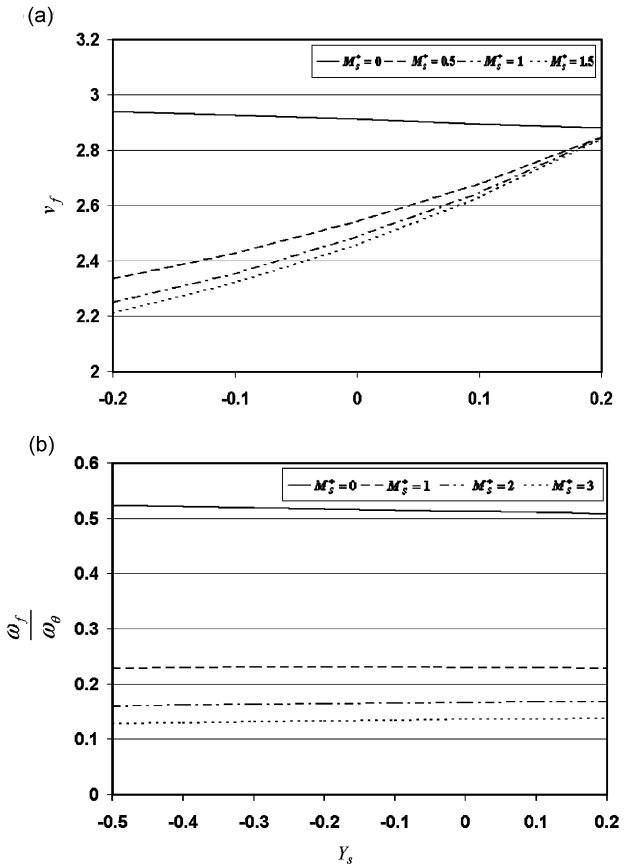

Fig. 9. Effects of the chordwise position of the follower force and external mass on the wing critical boundary for $X_s = 1$ and $p = 0.9$: (a) flutter speed and (b) flutter frequencies.

presence of the follower force, the critical location of the external mass from the point of dynamic stability, is the tip of the wing. This fact is independent of the store mass. Furthermore, in the case of the wing carrying no external mass (clean wing), but being subjected to the follower force, the spanwise location of the acted follower force does not influence the flutter frequency. This means that the location of the follower force is not important by itself in the determination of flutter frequency, but the store mass and its location affect flutter frequency significantly.

The influence of the chordwise location of the external mass on flutter speed and the frequency of the wing for different values of mass ratios is shown in Fig. 9. The external mass is located at the tip of the wing and the dimensionless follower force is $p = 0.9$. It is observed that the chordwise location of the external mass contributes different aeroelastic behavior for the wing with or without concentrated mass. Sliding the external mass toward the front of the wing will increase the flutter speed in the case of the wing carrying the tip mass subjected to the follower force. In the case of lack of external mass, for a clean wing subjected to a follower force, the flutter speed shows exactly the opposite behavior with respect to the chordwise location of the follower force; although this effect is very weak. As is shown in this figure, the flutter frequency is constant in the chordwise location of the external mass, but it is dependent, obviously, on its mass and increasing the tip mass leads to decreasing the flutter frequency.

Fig. 10 shows the effect of the non-dimensional chordwise location of the external mass on the wing flutter speed and frequency for selected values of the follower force acting on the tip weight with $M_s^* = 0.5$. This shows that the flutter speed increases by sliding the external mass toward the front of the wing. In addition, from this plot it is also possible to conclude the effects of the follower force on wing flutter speed. The results show a continued decrease in flutter speed accompanies the increase in the follower force, implying that the

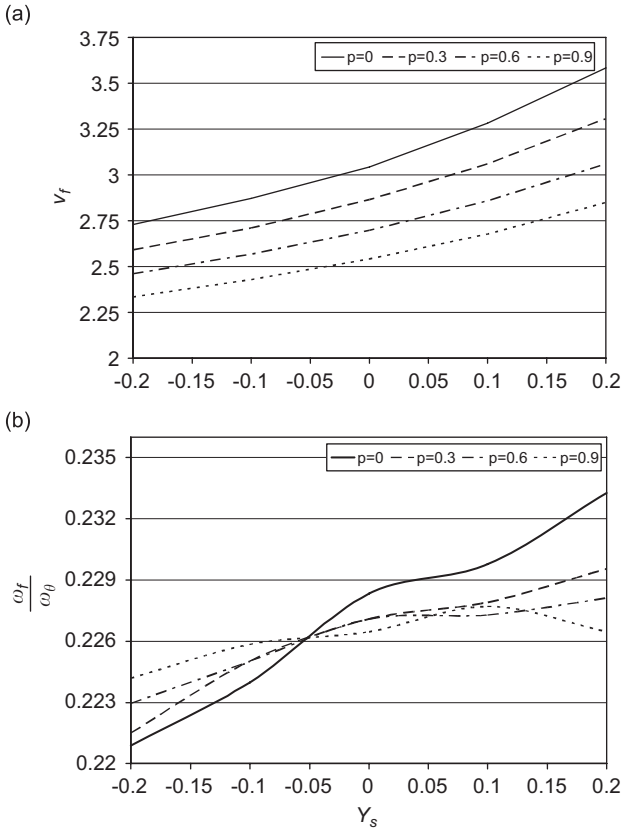

Fig. 10. Effects of the chordwise position of the follower force and external mass on the wing critical boundary for $X_s = 1$ and $M_s^* = 0.5$: (a) flutter speed and (b) flutter frequencies.

follower force decreases the flutter speed of the airplane. Sliding the external mass toward the front of the wing increases the flutter frequency in the case of $p = 0$. Increasing the p values weakens this effect, since for larger values of p the effects of the chordwise location of the attached mass and the follower force have no significant effects on the flutter frequency of the wing. It can be seen from the figure that for $p = 0.9$, flutter frequency shows exactly the opposite behavior with respect to the chordwise location of the follower force, mostly in the positive area of the diagram.

6. Conclusion

The purpose of this paper is the aeroelastic modeling and flutter analysis of a wing containing an arbitrarily placed mass subjected to a follower force. To this end, the complete aeroelastic equations for an isotropic aircraft wing carrying external mass, which is subjected to a follower force, are formulated by Hamilton's principle. The attached mass is considered to have offsets in three directions from the elastic axes of the wing, like a real aircraft engine or store, and the follower force is considered to act on the center of gravity of the external mass. These equations are valid for long, straight, homogeneous wings and are based on the rigidity of the attached external mass. In order to exactly consider the spanwise location and properties of the external mass and follower force the Dirac delta and Heaviside functions are used.

A parametric study of the follower force and the external mass magnitude and location on aeroelastic flutter is performed. Results are indicative of the important influence of the location and magnitude of the mass and the follower force on the flutter speed and frequency of the aircraft wing. The chordwise and spanwise locations of the mass and the magnitude of the follower force affect the stability region of the wing dramatically.

References

[1] V.V. Bolotin, *Non-Conservative Problems of the Theory of Elastic Stability*, Pergamon Press, Oxford, 1963.
[2] V.V. Bolotin, N.I. Zhinzher, Effects of damping on stability of elastic systems subjected to non-conservative forces, *International Journal of Solids and Structures* 5 (1969) 965–989.
[3] C.F. Kalmbach, E.H. Dowell, F.C. Moon, The suppression of a dynamic instability of an elastic body using feedback control, *International Journal of Solids and Structures* 15 (1974) 10–36.
[4] Q.H. Zuo, H.L. Schreyer, Flutter and divergence instability of non-conservative beams and plates, *International Journal of Solids and Structures* 33 (1996) 1355–1367.
[5] F.M. Detinko, Some phenomena for lateral flutter of beams under follower load, *International Journal of Solids and Structures* 39 (2002) 341–350.
[6] R.G. Nair, G.V. Rao, G. Singh, Stability of short uniform column subjected to an intermediate force, *Journal of Sound and Vibration* 253 (2002) 1125–1130.
[7] M. Goland, The flutter of a uniform cantilever wing, *Journal of Applied Mechanics* 12 (1945) 197–208.
[8] M. Goland, Y.L. Luke, The flutter of a uniform wing with tip weights, *Journal of Applied Mechanics* 15 (1948) 13–20.
[9] H.L. Runyan, C.E. Watkins, Flutter of a uniform wing with an arbitrarily placed mass according to a differential equation analysis and a comparison with experiment, NASA Technical Report, NACA TN 1848, 1949.
[10] I. Lottati, Aeroelastic stability characteristics of a composite swept wing with tip weights for an unrestrained vehicle, *Journal of Aircraft* 24 (1987) 793–802.
[11] F.H. Gern, L. Librescu, Static and dynamic aeroelasticity of advanced aircraft wings carrying external stores, *AIAA Journal* 36 (1998) 1121–1129.
[12] F.H. Gern, L. Librescu, Effects of externally mounted stores on aeroelasticity of advanced aircraft wings, *Journal of Aerospace Science and Technology* 5 (1998) 321–333.
[13] S. Na, L. Librescu, Dynamic response of adaptive cantilevers carrying external stores and subjected to blast loading, *Journal of Sound and Vibration* 231 (2000) 1039–1055.
[14] L. Librescu, O. Song, Dynamics of composite aircraft wings carrying external stores, *AIAA Journal* 46 (2008) 568–572.
[15] M. Como, Lateral buckling of a cantilever subjected to a transverse follower force, *International Journal of Solids and Structures* 2 (1966) 515–523.
[16] W.T. Feldt, G. Herrmann, Bending-torsional flutter of a cantilevered wing containing a tip mass and subjected to a transverse follower force, *Journal of the Franklin Institute* 297 (1974) 467–478.
[17] D.H. Hodges, Lateral-torsional flutter of a deep cantilever loaded by a lateral follower force at the tip, *Journal of Sound and Vibration* 247 (2001) 175–183.
[18] D.H. Hodges, M.J. Patil, S. Chae, Effect of thrust on bending-torsion flutter of wings, *Journal of Aircraft* 39 (2002) 371–376.

[19] D.H. Hodges, E.H. Dowell, Nonlinear equations of motion for the elastic bending and torsion of twisted non-uniform rotor blades. NASA Technical Report, NASA TN D-7810, 1974.
[20] E.H. Dowell, E.F. Crawley, H.C. Curtiss, D.A. Peters, R.H. Scanlan, F. Sisto, *A Modern Course in Aeroelasticity*, Kluwer Academic, Dordrecht, 1995.
[21] D.H. Hodges, G.A. Pierce, *Introduction to Structural Dynamics and Aeroelasticity*, Cambridge University Press, Cambridge, 2002.
[22] C.A.J. Fletcher, *Computational Galerkin Methods*, Springer, New York, 1984.